# SINGULARITY COMPUTATIONS

J. L. Swedlow

Report SM-76-6

October 1976

This paper was prepared as an invited lecture at the
International Symposium on Innovative Numerical Methods
in Applied Engineering Science
Versailles, 23-27 May 1977



Department of Mechanical Engineering
Carnegie Institute of Technology
Carnegie-Mellon University
Pittsburgh, Pennsylvania

# SINGULARITY COMPUTATIONS

J. L. Swedlow
Carnegie-Mellon University

One of the intriguing - and sometimes perplexing - classes of problems in mechanics involves singularities in otherwise smooth fields. Examples abound from the Joukowsky airfoil to Kelvin's problem and hardly need recounting here. Where an analytical solution is available, numerics may be simplified or avoided altogether. In other instances, numerical analysis is necessary, and properties of the singularity are then inferred from tabular information. These data are typically sparse or inaccurate in the immediate region of the singularity, or the numerical technique affords poor resolution, or some other impediment is encountered in establishing fully the result required.

Needed is an approach inherently untroubled by such shortcomings, one that indicates the structure of a singularity directly. In particular, it would be useful to have both the radial and angular (polar or spherical) distributions of the field quantities delineated as explicitly as is practicable, together with some measure(s) of the intensity of the singularity. In this paper, we suggest such an approach, based on recent development of numerical methods for elasto-plastic flow. This approach is patently applicable to other problems in solid mechanics and, without much effort, lends itself to certain types of heat flow, fluid motion, and the like.

Analytic solutions to classical problems in mechanics where a singularity occurs are divided, for our purposes, into two classes. In the first, one variable or set of variables is finite at the origin of the singularity, but

a second set - typically gradients - is not. Prime examples are displacements and strains at re-entrant corners, temperature and heat flux at an abrupt change in surface insulation. The second class involves singularities where none of the quantities is everywhere finite as, for example, in Kelvin's problem. This type of solution has proven essential to development of numerical procedures such as the boundary integral method and it thereby deserves close attention; because concern here rests with finite element methods in solid mechanics, where boundedness of displacements is necessary, we limit attention to just the first class of problem.

## PLANAR ELASTICITY

Singular behavior at re-entrant corners in classical planar elasticity (plane stress, plane strain) was fully articulated by Professor M. L. Williams [1] long before the widespread use of finite elements. His basic result in 1952 can be interpreted as the sum of two series, one of which provides the singularity in strain and stress, if such behavior exists for the geometry and boundary conditions prescribed. The second series gives regular results which, in the finite element sense, provide the components of rigid motion, "linear" displacements or "constant" strains, and increasingly higher order terms. This latter component of Williams's solution may be shown to be equivalent to the interpolation functions used commonly in regular finite elements.

There have been many developments reported in the literature to incorporate the first part of Williams's solution into finite elements for the specific case of a crack; see, e.g., [2,3]. Professor P. M. Quinlan has also used these functions to enhance an edge-function form of analysis [4],

and Dr. B. Gross and his colleagues have published a variety of solutions using collocation methods [5]. In all these instances, and in others where extraction of a stress intensity is the objective [6], it is essential to have at the outset a certain foreknowledge of the structure of the singularity. That is, were it not known from Williams - or an equivalent source - what to expect, none of these procedures could have been implemented.

Where information as to local behavior is desired, it is obvious that the details must be properly characterized either in advance or as an integral part of the (numerical) analysis. The case of planar elasticity is well in hand and no further primary findings are to be anticipated. For the purpose of our discussion, however, we make the supposition that the structure of the singularity - if, indeed, one were to exist - is not known and then enquire what steps might be taken to reveal that information. Knowing the basis of Williams's work as well as his results should then provide guidance for devising a numerical procedure.

Let us presume that, in some specific problem of interest, displacements in the vicinity of a suspected singularity behave in the following manner. In addition to rigid motion and linear variations in the displacement field which produce the familiar "constant" strains, the displacements along a ray from the origin (i.e., the point of singularity) behave as

$$u \sim \rho^q \quad . \tag{1}$$

where $\rho$ is a (linear) radial coordinate, and $q$ is an undetermined exponent. Let us furthermore focus on the case where $0 < q < 1$ to provide the type of problem in which we are interested, i.e., singular gradient(s) of u. It is noted that no regular element will produce the response shown in (1); while for some range of $\rho$ there may be a correspondence of regular element behavior and (1), the similarity is fortuitous and cannot be relied upon.

Our task now becomes that of finding q in (1), pertinent to some specific problem. In fact, the approach employed here addresses this task and is conceptually no different than that used in finite element analysis - we simply go a step further. An element is defined and its displacement field presumed as is usual, with terms of the form (1) included. Strains are computed, and the potential energy is defined and minimized with respect to nodal displacements; the result is the familiar stiffness equation. In a particular problem, however, solution strategy extends beyond solving the stiffness equation: potential energy is simultaneously minimized with respect to the exponent in (1) to achieve the full result.

To be more specific, we assume the re-entrant corner to be surrounded by an array of sectors which together comprise a special element, as in Figure 1. Arbitrarily here, each sector has five nodes as sketched and we assume the cartesian components of displacement take the form

$$\begin{aligned} u &= u_o + A_1 x + C_1 y + (E+F\theta)\rho^q \cos\theta - (G+H\theta)\rho^q \sin\theta \\ v &= v_o + D_1 x + B_1 y + (E+F\theta)\rho^q \sin\theta + (G+H\theta)\rho^q \cos\theta \end{aligned} \tag{2a}$$

Accordingly, the polar components of displacement are

$$\begin{aligned} u &= u_o \cos\theta + v_o \sin\theta + \tfrac{1}{2}(A_1+B_1)\rho + \tfrac{1}{2}(A_1-B_1)\rho\cos 2\theta \\ &\quad + \tfrac{1}{2}(C_1+D_1)\rho \sin 2\theta + (E+F\theta)\rho^q \\ v_\theta &= -u_o \sin\theta + v_o \cos\theta - \tfrac{1}{2}(C_1-D_1)\rho + \tfrac{1}{2}(C_1+D_1)\rho\cos 2\theta \\ &\quad - \tfrac{1}{2}(A_1-B_1)\rho \sin 2\theta + (G+H\theta)\rho^q \end{aligned} \tag{2b}$$

Clearly, $u_o$,$v_o$, and $(D_1-C_1)$ are rigid motions; further, $u_o$,$v_o$,$A_1$,,,H are coefficients to be determined (in terms of nodal displacements). The process of relating these coefficients to the nodal values, although tedious, is straightforward and the result is easily tabulated [7].

The "special" aspect of the element thus outlined is evident in the $\rho^q$ terms in (2). This simple representation is not more than an extension of the well-known constant strain element (CSE) and is thus but one of many possible configurations that one might contemplate for use in a given situation. For the present purpose, we take the element in Figure 1 to be embedded in an array of "regular" or unmodified CSEs which make up the structure to be analyzed as, for example, is shown in Figure 2. Some other possibilities are outlined in the Appendix.

The result of having evaluated the coefficients in (2) in terms of nodal displacements may be written

$$\{u\} = [\alpha(\rho,\theta)]\{\underline{u}\} \tag{3}$$

where $\{u\}$ represents the two components in (2a) and $\{\underline{u}\}$ is a vector of nodal displacement components. The matrix $[\alpha]$ is the set of interpolation functions; note that q appears only in $[\alpha]$. Following standard procedure, we next compute from (3) the strains

$$\begin{Bmatrix} \varepsilon_x \\ \varepsilon_y \\ \gamma_{xy} \end{Bmatrix} \equiv \{\varepsilon\} = [\beta(\rho,\theta)]\{\underline{u}\} \tag{4}$$

as a precursor to computing the potential energy of the entire element assembly. In this context, note that (3) and (4) pertain to a typical sector of the special element, so that the potential energy will involve a summation of the contributions from each sector.

Since

$$\therefore \quad \begin{Bmatrix} \sigma_x \\ \sigma_y \\ \tau_{xy} \end{Bmatrix} \equiv \{\sigma\} = [M]\{\varepsilon\}$$

we have the potential energy for the typical sector as

$$U_s = \frac{1}{2}\{\underline{u}\}^T \int_{\theta_1}^{\theta_2} \int_{o}^{2\rho_e} [\beta]^T [M][\beta]\rho d\rho d\theta \{\underline{u}\} - \{\underline{u}\}^T \int_{S_\sigma} [\alpha]^T \{t\} dS \tag{5}$$

where $\{t\}$ is the traction vector specified on some part $S_\sigma$ of the sector's boundary S. Summing terms of the form (5) over the sectors, we arrive at the special element's potential energy

$$U_e = \sum_s U_s$$

in which many of the traction terms obviously cancel. We next add the potential energies of each of the regular elements $U_r$ to arrive at the total value for the system:

$$U = U_e + \sum_r U_r \tag{6}$$

To the extent that the surfaces of the re-entrant corner are traction-free or, alternatively, that their nodal displacement components are specified, the only uncancelled contributions to the overall system's traction are precisely where tractions are specified, normally far from the re-entrant corner.

We are now prepared to minimize the functional U with respect to nodal displacements, arriving at the familiar stiffness equation. In the present development, the entries in the stiffness matrix take the same form for regular (CSE) elements as has been shown in many places. The contribution from each sector of the special element derives from the first integral in (5) and, together, a stiffness for the special element may readily be identified. Even with this relation, however, it is clear that no constraint on the expo-

nent q has obtained; indeed, solving the stiffness equation could go forward with virtually any value for q. Were q somehow known, however, the computation at this stage is unremarkable except for (what appears to be) some negligible incompatabilities between the special and regular elements.

The constraint on q, so far lacking, is obtained by minimizing the functional U with respect to the exponent itself. Were we to set $\partial U/\partial q = 0$, however, the result would be an hideously non-linear equation to be handled along with the stiffness equation. It is apparent from (6) that minimization of U with respect to q is equivalent to minimization of $U_e$, since $U_r$ is not functionally dependent upon q. Hence, if the result of minimizing U with respect to all nodal displacements {u} is the familiar stiffness equation

$$[K]\{u\} = \{T\}$$

we have the simultaneous statement

$$U_e = \text{minimum with respect to } q \tag{7b}$$

Together, (7a) and (7b) pose the problem fully for prescribed nodal forces {T}.

It is well at this point to comment on the connection between this formulation and that employed by Williams [1], so that the equivalence emerges. It will be recalled that Williams employed the Airy stress function $\chi(\rho,\theta)$ in the form

$$\chi(\rho,\theta) = \rho^{\lambda+1}F(\theta;\lambda) \tag{8}$$

and required $\chi(\rho,\theta)$ to be a biharmonic function. This led to an ordinary differential equation for $F(\theta;\lambda)$ whose solution gave the proper dependence on $\theta$, with four constants of integration, but left $\lambda$ unspecified. Williams argued that $\lambda > 0$ is necessary to provide finite displacements as $\rho \to 0$ (since the displacement components were demonstrably $O(\rho^{\lambda})$), and that $0 < \lambda < 1$ would lead to singularities in strain and stress. To determine $\lambda$, Williams invoked sets of boundary conditions at $\theta = \theta_o$ and $\theta = -\theta_o$ (see

Figure 1); these sets of conditions were limited to the surfaces of the re-entrant corner being clamped (zero displacements) or free (zero tractions). The four conditions (two at $\theta_o$ two at $-\theta_o$) for the four constants of integration are thus homogeneous; the necessary condition for their solution yields an eigenequation for $\lambda$. The result, especially for a crack ($\theta_o = \pi$), has been used repeatedly in mechanics as noted above.

If, alternatively, Williams had begun by writing displacements in the form

$$\begin{aligned} u_\rho &= \rho^\lambda f(\theta;\lambda) \\ v_\theta &= \rho^\lambda g(\theta;\lambda) \end{aligned} \tag{9}$$

and required the stresses derived from (9) to *satisfy the equations of equilibrium*, the eventual result would be identical to his published findings. What is done here, of course, follows an alternate procedure which results in one significant difference. The representation (2) is not required to satisfy equilibrium at an arbitrary point $(\rho,\theta)$ but is forced to do so *over a finite region*, here, the sector. That is, the result of minimizing U imposes equilibrium element-(or sector-) wise and not point-wise.

As to the boundary conditons, *there is no difference*. Were (2) inserted into an analytic development based on minimum potential energy, the same boundary conditions as used by Williams would obtain. Thus the exponent q in (2) is subject to precisely the same constraint Williams obtained for $\lambda$ in (8), or would have obtained for $\lambda$ in (9).

What the present formulation then provides is an approximate statement of interior equilibrium and an effectively exact boundary condition. The interior approximation is perforce tailored to the form of the assumed displacement components, whether they be (2) or (9) or forms suggested in the Appendix. The boundary constraint, however, is identical to that in Williams's eigenequation. It may be noted further that Williams's argument for the finiteness of displacement as $\rho \to 0$ is here replaced by boundedness of

of the potential energy, a condition familiar to numerical analysts and, in certain respects, more easily treated.

Returning to the problem statement (7), we comment on a solution tactic. Both (7a) and (7b) must be satisfied, and it appears straightforward to proceed on an iterative basis. Let us assume a reasonable starting value for q and solve the linear equations in (7a) in the same manner as used in dealing with standard finite element problems. Arriving at a set of nodal displacements, the function $U_e$ is minimized with respect to the exponent q. Note that since nodal displacements are fixed, $S_\sigma$ in (5) is null and the minimization proceeds on the first integral in (5), summed over all sectors of the special element. A new value of q is found and (7a) is solved again. The process continues until both (7a) and (7b) are satisfied to whatever degree of precision is appropriate to the computation and the computer involved. Having thus converged, the solution, in terms of {u} and q, is in hand. Straightforward data reduction will provide both the full structure of the singularity, at least within the precision of (2), and the intensity of the singularity for the problem of interest.

## SOME SIMPLE EXTENSIONS

The formulation outlined above may be extended to allied problems. The inclusion of body forces due, for example, to gravitational or centrifugal loading (as in a spinning disc) is effected merely through adding appropriate terms to the potential energy in (5) and (6). Thermal excitation is included in an analogous manner. Dynamic behavior is modeled by replacing the theorem of minimum potential energy by Hamilton's principle. Such extensions in ordinary planar elasticity are theoretically well founded [8] and operational in a number of existing codes.

Another type of extension to the foregoing development is equally obvious. Material anisotropy is incorporated via simple changes in the matrix [M]. Spatial variation in material properties may also be incorporated by appropriate alterations to [M], although the analyst should take note of the spatial gradients in [M] when designing an element map. With due caution, then, problems of the sort considered by Hein and Erdogan [9], for example, may be treated by finite elements.

## NON-LINEARITIES

To this point, we have done little more that show an alternate technique for replicating the basic information contained in Williams's eigenanalyses. While his findings give a basis for demonstrating and substantiating the present approach, its utility derives from circumstances where an eigenanalyses does not exist or is available solely through highly idealized modeling.

Non-linear behavior is a case in point. If we consider first material non-linearity due to yield, we observe that the only analytic result available is the so-called HRR model [10]. This situation pertains to planar behavior, as does Williams's work, but is limited in certain respects. It admits plastic deformations only, it idealizes the material, and results presently available pertain only to a crack and not to the general re-entrant corner. Since in large measure the effect of yielding (or plastic flow, or non-linear material response) is to alter the initial singularity, it would be most useful to know how the change proceeds from the outset. That is, there may be significant technological interest in the process (as well as its rate of progress) whereby the material goes from the one limiting case described by Williams to the other limit characterized by the HRR model.

We have given considerable attention to this issue, and results are just now coming to hand. A preliminary discussion appears elsewhere [11], and further documentation is anticipated, e.g., [12]. For the present discussion a brief outline of the formulation is in order. The steps described above are followed except that (3) is replaced by

$$\{\delta u\} = [\alpha(\rho,\theta)]\{\delta \underline{u}\}$$

where the $\delta$ signifies an increment in each of the various displacement components. Then (4) becomes

$$\{\delta \epsilon\} = [\beta(\rho,\theta)]\{\delta \underline{u}\}$$

and since the flow rule for elasto-plastic flow is written

$$\{\delta \sigma\} = [M]\{\delta \epsilon\}$$

one needs only an analogue to (5) to carry the analysis through. The required theorem is in fact available [13] and we write for (7)

$$[K]\{\delta u\} = \{\delta T\} \tag{10a}$$

$$U_e = \text{minimum with respect to } q \tag{10b}$$

The problem (10) is to be solved successively for the incremental values of the displacement components, not their accumulated or current values. This problem is linear in the increment - in the sense that (7) is linear - and the procedure for its solution is established [14].

Certain matters relating to implementation are to be noted. One must choose the radial extent of the special element, the number of sectors used, and the refinement within each sector needed to effect proper quadrature. To investigate these matters, extensive evaluation of the code was performed using elementary solutions (as in [1]) as a basis. No clear criteria for sizing the element, i.e., fixing $\rho_e$, emerged except where a relationship could be established *a priori* by a given set of loading conditions. Circumferential

behavior, on the other hand, could easily be seen to improve with increasing numbers of sectors, at least for the simple formulation (2). It does appear from work in progress [15] that a more refined representation behaves in the same manner, reaching acceptable performance with a modest number of sectors ($\sim$ 10). For the element described in (2), however, we chose 48 sectors for $-\pi < \theta < \pi$ as the best trade-off between angular resolution and storage requirements*. Quadrature was evaluated using a number of techniques; while the first integral in (5) is always bounded, it contains non-analytic function of $\rho$ which impede a formal prediction of the behavior of various methods. In the event, we chose Gaussian quadrature with three angular positions in $\theta_1 < \theta < \theta_2$ and seven in $0 < \rho < 2\rho_e$. Good accuracy was obtained for various values of q in (2); other combinations may become preferred in other models, e.g., as described in the Appendix.

The residual issue of sizing the radial extent of the special element was resolved empirically. For the center-cracked configuration of [11], we examined the elastic potential energy of the test specimen as $\rho_e$ was reduced, finding that a stationary value obtained for $\rho_e \sim 0$ (crack length/100). While surely this result reflects both the modeling in (2) and numerical precision of the computation itself, it also provides confidence in the element mapping. Having thus arrived at a suitable element array, an elasto-plastic analysis for a configuration reported earlier [16] proceeded; in this manner distinct results for the same problem were available to ensure that the special element computations could be corroborated. Other problems have since been considered and results are to be reported shortly [12,15]. It is of interest here, however, to note one or two aspects of the solution in [11]. Data

*Actually, analyses were performed for a symmetric configuration so that 24 sectors were employed for the half specimen.

were presented for four load levels:

purely elastic response;

yield detected just beyond the special element, denoted as load step 38;

yield extended through the cross-section, denoted as load step 73; and

average applied stress exceeded the yield point, denoted as load step 93.

The radial variation of the octahedral or an effective stress, normalized on the respective value of yield, is shown in Figure 3 for one angular position. Radial variation of $u - u_o$ and v, normalized on the uniform far-field extension $\Delta$, is shown in Figure 4*. Angular distributions of the same quantities appear in Figures 5 and 6. Note that the elastic results which exhibit high gradients are smoothly described; at high yield levels, roughness develops in some of the data. Nonetheless, one is able even with a crude representation of the type given in (2) to infer a fair sense of the structure of the crack tip's singularity as yield proceeds. Incidentally, it may also be remarked that the analysis compares favorably to the experimentally observed specimen behavior for which a companion analysis was performed earlier [16].

As a second item, geometric non-linearity may be incorporated in the analysis. While the one analytic solution [17] to the problem confirms a localized singularity, it is necessarily confined to a specialized material representation. The obvious issues then become, for a more arbitrary material characterization, the degree to which the sharp corner blunts and the size scale over which this event occurs as loading proceeds. Dr. J. R. Osias has investigated this matter using conventional elements in his original Eulerian formulation [18]. More recently, he has reformulated the problem for a special

*Nomenclature is the same as that used in (2a); for reasons of symmetry $v_o = 0$.

element of the type considered here, necessarily using a Lagrangian coordinate frame [19]. In this manner, the radial coordinate whose exponent is to be determined is readily identified.

It is useful to touch briefly on the field problem. The initial domain $B_o$ is bounded by $S_o$ and, as above, tractions are specified on $S_\sigma$. Using conventional indicial notation, coordinates, displacements, and velocities in $B_o$ are described by $X^I$, $U^I$, and $V^I$, respectively; coordinates in the deformed domain B are $x^i$. Large strain elasto-plastic behavior is governed by quasi-static rate equations of the form

$$\dot{S}^{IJ} = P^{IJKL}\dot{E}_{KL}$$

where $\dot{S}^{IJ}$ is the convected Kirchhoff stress rate and $\dot{E}_{IJ}$ is the material derivative of Green's strain, viz.,

$$\dot{E}_{IJ} = \frac{1}{2}(V_{I;J} + V_{J;I} + U^K_{;I}V_{K;J} + U^K_{;J}V_{K;J})$$

Finally, $P^{IJKL}$ is a constitutive tensor which is created to coincide with Hooke's law for small elastic deformations but subsequently accommodates arbitrary work-hardening material behavior, including provision for unloading and reloading. The stationary principle developed by Osias [19] is then

$$\Pi = \frac{1}{2}\int_{B_o}\{P^{IJKL}\dot{E}_{IJ}\dot{E}_{KL} + S^{KL}V^I_{;K}V_{I;L}\}dB - \int_S \dot{T}^I V_I dS \qquad (11)$$

$$\delta\Pi = 0$$

where $\dot{T}^I$ are the traction rates specified on $S_\sigma$. With (11) one needs only to design an element and its interpolation functions, as above, to arrive at the analogue to (7) or (10).

Osias, however, adds a further refinement which may surely be adapted to the elements discussed elsewhere. Because of the need to identify the size scale of the event*, the effective range of terms of the form (1) is also

*This matter may be visualized as the relation between the effective radius of the blunted corner and that of the special element, which alters as excitation progresses: This radius should remain somewhat smaller than that of the element.

considered to be a variable. Hence the approach is to define first the base element to be used in the host program, and then to overlay the appropriate counterpart of Figure 2 with special functions. For example, Figure 2 could be supposed to represent six-noded triangles. The sectors comprising the special element contain as a part* of their total interpolation functions displacement distributions given by

$$U_I(R,\Theta) = \mathcal{R}_I(R/R_S,\Theta)\,\vartheta_I(\Theta-\bar{\Theta}) \text{ (no sum on I)} \tag{12}$$

where $R_S \leq R_e$ is the relation between the range $R_S$ over which (12) is operative and the (Langrangian) radius measure of the sector; $\Theta_1 \leq \Theta \leq \Theta_2$ is the angular coordinate, with $\bar{\Theta} = (\Theta_1 + \Theta_2)/2$; and the functional forms $\mathcal{R}_I$ and $\vartheta_I$ remain to be specified. Clearly (12) is operative only for $R/R_S \leq 1$ and will contain $(R/R_S)^q$; Osias observes that $U_I$ and its gradients must vanish smoothly as $R/R_S \to 1$. An example is suggested but not implemented in [19]; the point of interest here is not so much the detail as the fact that computation of a singularity may proceed in the context of geometric non-linearity. It is moreover evident that material and geometric non-linearities may be treated together [18,19] as a more physically realistic model than the more familiar linear elastic case.

It may also be remarked that the present approach admits a feature in modeling not elsewhere considered. We know from a variety of sources that plastic flow and blunting occur at a sharp, re-entrant corner, but that these events tend to have a directional character. That is, for example, the degree of yield varies with $\theta$(or $\Theta$). It is therefore not obvious that the exponent q in (1) or (2) should be invariant with respect to the angular coordinate. The present formulation allows the exponent to vary so that, for a crack, the relatively inactive zones tending to lie ahead of the crack and along its flanks

*See Appendix 1 for one means for overlaying regular behavior with a special distribution.

may more realistically be modeled. Osias accounts for this situation [19], as did we originally [7], but there is some computational cost involved in having a larger number of variables in the statement (7b). Nonetheless, the analyst retains the option to examine directionality of non-linear behavior which, for some circumstances, may prove useful [15].

## AXISYMMETRY

The very familiarity of linear elasticity has the virtue of facilitating consideration of more complex circumstances. So far the discussion has been in the context of planar problems owing largely to Williams's original findings. It is known that non-planar crack problems have been solved [20], and the question naturally arises whether the structure of this singularity relates to the planar form. While correspondence has been demonstrated for a crack, there is evidence to suggest that the intensity may depend on far-field geometry or other features not immediate to the crack's tip or edge [21].

An analogue to Williams's planar eigenanalyses would be the obvious step for the axisymmetric case. Consideration ought not to be limited to cracks, however, as there are other configurations of technical interest. These include piping flanges, step changes in shaft diameter, and sudden thickness variations in thick shells. Unfortunately, the Williams type of analysis does not go forward as in the case of planar behavior, because the governing equations do not admit a product solution [22]. These equations, for the configuration shown in Figure 7, derive from the simple transformation

$$r = R + \rho \cos(\psi + \psi_o), \quad z = Z + \rho \sin(\psi + \psi_o) \tag{13}$$

in the $(\rho,\theta,\psi)$ coordinates, displacements are $(\xi,\eta,\rho)$; the strains are

$$
\begin{aligned}
\varepsilon_\rho &= \partial\xi/\partial\rho \\
\varepsilon_\theta &= (\partial\eta/\partial\theta + \xi r_\rho + \zeta r_\psi/\rho)/r \\
\varepsilon_\psi &= (\partial\zeta/\partial\psi + \xi)/\rho \\
\gamma_{\theta\psi} &= (\partial\eta/\partial\psi)/\rho + (\partial\zeta/\partial\theta - \eta r_\psi/\rho)/r \\
\gamma_{\psi\rho} &= \partial\xi/\partial\rho + (\partial\xi/\partial\psi - \zeta)/\rho \\
\gamma_{\rho\theta} &= \partial\eta/\partial\rho + (\partial\xi/\partial\theta - \eta r_\rho)/r
\end{aligned}
\tag{14}
$$

and equilibrium is written as

$$
\begin{aligned}
&\partial\sigma_\rho/\partial\rho + (\sigma_\rho - \sigma_\theta) r_\rho/r + (\sigma_\rho - \sigma_\psi)/\rho + (\partial\tau_{\rho\theta}/\partial\theta)/r \\
&\quad + (\partial\tau_{\rho\psi}/\partial\psi)/\rho + \tau_{\rho\psi}(r_\psi/\rho)/r = 0 \\
&\partial\tau_{\rho\theta}/\partial\rho + (1/\rho + 2r_\rho/r)\tau_{\rho\theta} + (\partial\sigma_\theta/\partial\theta)/r + (\partial\tau_{\theta\psi}/\partial\psi)/\rho \\
&\quad + 2\tau_{\theta\psi}(r_\psi/\rho)/r = 0 \\
&\partial\tau_{\rho\psi}/\partial\rho + (r_\rho/r + 2/\rho)\tau_{\rho\psi} + (\partial\tau_{\theta\psi}/\partial\theta)/r + (\partial\sigma_\psi/\partial\psi)/\rho \\
&\quad + (\sigma_\psi - \sigma_\theta)(r_\psi/\rho)/r = 0
\end{aligned}
\tag{15}
$$

In (14) and (15) we use the notation

$$r_\rho = \cos(\psi+\psi_o), \quad r_\psi/\rho = -\sin(\psi+\psi_o)$$

For axisymmetry, $\partial/\partial\theta$ is a null operator and (14) (15) decouple to two sets, one for extension and one for torsion in which

$$\xi = \xi(\rho,\psi), \quad \eta = 0, \quad \zeta = \zeta(\rho,\psi) \quad \text{and} \quad \xi = 0, \ \eta = \eta(\rho,\psi), \quad \zeta = 0$$

For extension, functions of the Neuber-Papkovich type may be introduced after consideration of the coordinate transformation [22]; denoting these as $\omega$ and $\vartheta$, we find

$$2\mu\xi = -\partial\omega/\partial\rho + (3-4\nu)\vartheta - [\rho+R\cos(\psi+\psi_o)]\partial\vartheta/\partial\rho$$

$$2\mu\zeta = -(1/\rho)\partial\omega/\partial\psi - [1+(R/\rho)\cos(\psi+\psi_o)]\partial\vartheta/\partial\psi + [(R/\rho)\sin(\psi+\psi_o)]\vartheta$$

The corresponding differential equations are decoupled but awkward so that we introduce

$$\Lambda = (\sqrt{r})\omega$$

$$\Theta = (\sqrt{r})\vartheta$$

to find

$$\partial^2\Lambda/\partial\rho^2 + (1/\rho)\partial\Lambda/\partial\rho + (1/\rho^2)\partial^2\Lambda/\partial\psi^2 + (1/4r^2)\Lambda = 0$$

$$\partial^2\Theta/\partial\rho^2 + (1/\rho)\partial\Theta/\partial\rho + (1/\rho^2)\partial^2\Theta/\partial\psi^2 \qquad (16)$$

$$+ [(1/4-r_\rho^2)/r^2-1/\rho^2]\Theta = 0$$

as the equations of interest. (Forms similar to the first of (16) obtain for torsion.) The presence of both $\rho$ and $r$ in the denominators of the coefficient in the various terms of (14), (15), and (16) precludes the "separation of variables" approach inherent in (8) or (9), and the template for solution provided by Williams fails*. It is, of course, possible to assume $\rho << R$ and integrate (16) in terms of Bessel functions, seeking asymptotic forms for small $\rho$. Such an approach, however, is objectionable for two reasons. The solution is approximate and equilibrium is not fully satisfied. Further, the degree of approximation remains unestablished and there may be errors at the boundary itself. Second, such a solution is not useful in procedures already developed for such problems including ordinary special elements, e.g., [2,3], edge functions [4], and collocation [5]; one is left with finite elements as in [21].

*We have also examined formulations including the Galerkin vector and its special form, Love's strain function; Southwell functions, both as originally stated [23] and as modified by Zak [24]; and the Maxwell-Morera functions. Of these, the procedure shown is the most promising.

If we must settle for approximate solutions, it seems sensible to adjust the approximation to the particular problem. Thus we prefer an approach which is patterned after that outlined in this paper. The analogue to (2) becomes simply

$$u_r = u_o + A_1 r + C_1 z + (E+F\psi)\rho^q \cos(\psi+\psi_o) - (G+H\psi)\rho^q \sin(\psi+\psi_o)$$
$$w_z = w_o + D_1 r + B_1 z + (E+F\psi)\rho^q \sin(\psi+\psi_o) + (G+H\psi)\rho^q \cos(\psi+\psi_o) \tag{17a}$$

and

$$\xi = u_o \cos(\psi+\psi_o) + w_o \sin(\psi+\psi_o) + \tfrac{1}{2}(A_1+B_1)\rho + \tfrac{1}{2}(A_1-B_1)\rho \cos[2(\psi+\psi_o)]$$
$$+ \tfrac{1}{2}(C_1+D_1)\rho \sin[2(\psi+\psi_o)] + (E+D\psi)\rho^q$$
$$\eta = -u_o \sin(\psi+\psi_o) + w_o \cos(\psi+\psi_o) - \tfrac{1}{2}(C_1-D_1)\rho + \tfrac{1}{2}(C_1+D_1)\rho \cos[2(\psi+\psi_o)] \tag{17b}$$
$$- \tfrac{1}{2}(A_1-B_1)\rho \sin[2(\psi+\psi_o)] + (G+H\psi)\rho^q$$

Using (14), the strains are found and the procedure of computing and minimizing potential energy is followed, directly in analogue to the foregoing discussion.

As has been observed by many authors, probably first by Irwin [25], the singularity for a crack geometry is expected to be the familiar value $q = 1/2$. What is not known, however, is the result for geometries associated with a flange, a change of section, layered materials, and so on. That is, what is $q(R,\alpha,\psi_o)$? To the extent that such information is of technical interest, either for use in other computations (e.g., [3,4]) or for specific applications, the foregoing development appears to be the first direct means available for establishing the structure of an elastic singularity at a re-entrant corner in an axisymmetric geometry.

Moreover, it is evident from the work now in progress (which deals with non-linearities in planar situations) that the procedure carries over directly

to non-linearities in the axisymmetric case. In the same sense that finite elements are used in both planar and axisymmetric analyses, extension of the formulation in (17) is appropriate to elasto-plastic flow [14] and to large deformations [18,19]. For these situations, the nature of the singularity may be established numerically and perhaps in no other manner.

## THREE DIMENSIONS

The numerical approach described here is fully pertinent to three-dimensional problems. The context is a vertex formed by intersection of three surfaces, and two simple examples are sketched in Figure 8. Further examples may be drawn from the literature in crack problems, where a crack intersects a free surface. The crack front may be straight or curved, and the intersection need not be normal to the free surface. Some possibilities were outlined earlier [21], and Dr. B. K. Neale has recently reported a series of such observations [26]. From experimental sources, the inference of a singularity peculiar to the vertex itself is not uncommon, and Professor E. S. Folias has made an initial analytic extraction of such behavior [27]. The highly resolved numerical results developed by Dr. T. A. Cruse are also supportitve of the notion of a vertex singularity [28].

Such information is appropriate to the computational approach outlined here. It is easy to envisage the shapes sketched in Figure 8 filled with polygonal cones whose apices all coincide at the vertex of the corner. A radial coordinate from that point becomes $\rho$ in (1). The question then becomes how the displacements vary with this radial coordinate. There will of course be rigid motion, and one must also allow for constant strains in the usual manner. Obviously, however, behavior of the sort suggested by (1) can intrude as well; information of the sort outlined above suggests that inclusion of

terms of the form (1) is most appropriate. As a result, one may infer a process of modeling which will explicitly account for a vertex singularity. Furthermore, one may study behavior along an edge (intersection of two surfaces) by the same means and examine, among other points, structure of the singularity as a function of the shape of the edge.

It would be tedious here to write the equations of elasticity in spherical coordinates centered at the vertex, and to expand them for elementary interpolation functions for, say, a tetrahedron or a pyramid*. Obviously enough, such development is straightforward if lengthy to carry out, and it could be implemented in terms of code. We prefer instead to emphasize that the discussion following (9) is immediately applicable. Minimization of the potential energy yields an approximate statement of equilibrium (sectorwise as opposed to point-wise) and effectively exact boundary conditions. To the extent that the exponent on the radial coordinate is an artifact of these boundary conditions and not the field equations, the analyst may anticipate determination of the vertex singularity to a considerable degree of accuracy. Moreover, the singularity computation is direct and explicit, and it should reveal the structure of the singularity without need for extensive data reduction.

## CONCLUDING REMARKS

We have sought to describe an approach for singularity computations which is based on a primary concept in mechanics. The procedure replicates the conditions used for the same purpose in more formal analysis, as applied to planar configurations, but is in no manner limited to linear or elastic or small strain or two-dimensional situations. Rather, the range of cir-

*That is to say, a triangular cone or a rectangular cone.

cumstances for which the approach may be used appears to be unlimited, and it evidently carries over to other classes of problems such as heat flow. As a result, there is now an opportunity to attack problems which so far have proven difficult in the sense that details of the singularity's structure are not yet well articulated. While this approach requires more extensive preparation prior to implementation and additional computation costs are encountered, the directness of obtaining results needed for certain research objectives would appear to make this approach worthy of use in serious singularity computations.

ACKNOWLEDGMENT

The work leading to preparation of this paper was sponsored by the National Aeronautics and Space Administration, under NASA Research Grant NGR 39-087-053. We are grateful for this continuing support and for fruitful discussions with Drs. J. R. Osias and J. E. Srawley, and Messrs. M. E. Karabin, Jr., and C. Marino. Consultation with faculty of Imperial College of Science and Technology has also proven useful, and it is a pleasure to acknowledge these discussions.

## APPENDIX - ADDITIONAL INTERPOLATION FUNCTIONS

The element formulation in (2) exemplifies the basic approach needed to exploit (1) in the sense of an undetermined exponent. By no means, however, is the procedure limited to the primitive form in (2). Much more substance can be incorporated in the interpolation functions, but there are evident constraints to be observed. Noting that (1) derives from a certain physical sense of the solution's behavior, one must guard against the use of coordinates whose physical interpretation is not clearly understood. Thus, for example, use of isoparametric elements is problematic unless the internal coordinate(s) can be directly identified with the radial coordinate of interest. Indeed, Freese and Tracey [29] recently noted the sensitivity of elastic behavior in crack problems to overall element shape.

It appears therefore advisable to work with physical coordinates when formulating an element, or to use an isoparametric form in which the physical coordinates are manifest. Marino, in work soon to be documented, employs the latter method with evident success [15]. An example of the former is suggested in Figure 9 and a more complex version of (2) as follows:

$$\begin{aligned} u = {} & u_o + A_1 x + A_2 x^2 + C_1 y + C_2 y^2 + Exy \\ & + [G_o + G_1(\theta-\bar{\theta}) + G_2(\theta-\bar{\theta})^2]\rho^p \cos\theta \\ & - [H_o + H_1(\theta-\bar{\theta}) + H_2(\theta-\bar{\theta})^2]\rho^q \sin\theta \\ v = {} & v_o + D_1 x + D_2 x^2 + B_1 y + B_2 y^2 + Fxy \\ & + [G_o + G_1(\theta-\bar{\theta}) + G_2(\theta-\bar{\theta})^2]\rho^p \sin\theta \\ & + [H_o + H_1(\theta-\bar{\theta}) + H_2(\theta-\bar{\theta})^2]\rho^q \cos\theta \end{aligned} \qquad (18a)$$

where $\bar{\theta} = (\theta_1+\theta_2)/2$. It follows that

$$u_\rho = u_o \cos\theta + v_o \sin\theta + \tfrac{1}{2}(A_1+B_1)\rho + \tfrac{1}{2}(A_1-B_1)\rho\cos 2\theta$$
$$+ \tfrac{1}{2}(C_1+D_1)\rho\sin 2\theta + \tfrac{1}{2}(A_2+C_2+F)\rho^2\cos\theta$$
$$+ \tfrac{1}{2}(A_2-C_2-F)\rho^2\cos\theta\cos 2\theta + \tfrac{1}{2}(B_2+D_2+E)\rho^2\sin\theta$$
$$+ \tfrac{1}{2}(B_2-D_2-E)\rho^2\sin\theta\cos 2\theta + [G_o + G_1(\theta-\bar{\theta}) + G_2(\theta-\bar{\theta})^2]\rho^p \qquad (18b)$$
$$v_\theta = -u_o \sin\theta + v_o \cos\theta - \tfrac{1}{2}(C_1-D_1)\rho + \tfrac{1}{2}(C_1+D_1)\rho\cos 2\theta$$
$$- \tfrac{1}{2}(A_1-B_1)\rho\sin 2\theta - \tfrac{1}{2}(A_2+C_2-F)\rho^2\sin\theta$$
$$- \tfrac{1}{2}(A_2-C_2-F)\rho^2\sin\theta\cos 2\theta + \tfrac{1}{2}(B_2+D_2-E)\rho^2\cos\theta$$
$$- \tfrac{1}{2}(B_2-D_2-E)\rho^2\cos\theta\cos 2\theta + [H_o+H_1(\theta-\bar{\theta}) + H_2(\theta-\bar{\theta})^2]\rho^q$$

Note that two exponents are allowed in this representation, one for each of the polar components of displacement. The remainder of the expression is based on the notion of a linear strain element (LSE). In that context, note that an eight-noded element obtains by omitting the $G_2$ and $H_2$ terms in (18b) or perhaps the E and F terms in (18a). We could, in addition, let the exponents vary in the angular direction, i.e., $p,q = p(\theta),q(\theta)$, but care must be exercised to avoid intersector incompatabilities.

A feature of re-entrant corner and crack problems, sometimes overlooked, is that circumferential gradients of strain and stress can be greater than radial gradients. This may be observed most simply by plotting contours of selected field quantities, as in [30], and noting behavior in the respective directions. One may also use this as a basis for sizing the special element, or its effective radial range. Alternatively, an energy basis may be used as described in the main part of the paper.

Other formulations may be generated in this intuitive manner, each of which should be evaluated for its efficacy with respect to the problem type anticipated. It is not so much our purpose here to devise an optimal element - that condition appears to be problem dependent - but we do note that formulation

may proceed independently of the overall conceptual framework. In that context, we should note the procedure termed "singularity programming" devised by Emery and his colleagues [31]. This formulation involves superposing special or irregular behavior on an established element by writing

$$\{u\} = [R]\{A\} + k\{S\} \tag{19}$$

Here, {u} has the same meaning as in (3); [R] is a matrix of regular, typically analytic, interpolation functions as in the CSE, LSE, or isoparametric representation; {A} is a vector of constants; k is a scale factor; and {S} is a vector of interpolation functions which contain the exponent q and represent the special aspects of the element. Evaluating {u} at the nodes leads to the vector $\{\underline{u}\}$; (19) is solved for {A} and rewritten as

$$\{u\} = [N]\{\underline{u}\} + k\{S\}$$

where

$$[N] = [R][R]^{-1}$$

$$\{S\} = \{S\} - [N]\{\underline{S}\}$$

Clearly {S} vanishes at the nodes; it does, however, interact with the nodal excitation as may be seen by carrying through development of the stiffness equation. The formulation is interesting in that, while it allows determination of the exponent(s) in {S}, the magnitude of the special behavior is scaled by the single factor k. Hence one must either be more specific as to the angular variation, relative to what is permitted in (18), or settle for possibly a stiffer element. In addition, since the potential energy is minimized with respect to k, there are entries in the stiffness equation beyond the usual terms, whereas the formulations (2) and (18) do not present such an inconsistency. Whatever admissible formulation is used (see also [32]), the option of adjusting the singular structure remains available and the analyst must choose ultimately in terms of the problem class he faces.

## REFERENCES


1. Williams, M. L., *Journal of Applied Mechanics* 19 (1952) 526-530; 24 (1957) 109-114; 28 (1961) 78-82.

2. Byskov, E., *International Journal of Fracture Mechanics* 6 (1970) 159-167.

3. Wilson, W. K., in *Stress Analysis and Growth of Cracks*, STP 513, American Society for Testing and Materials, Philadelphia (1972) 90-105.

4. Quinlan, P M., *Proceedings of the Royal Irish Academy* 64 series A 1965); in *Studies in Numerical Analysis*, Academic Press, New York (1974) ; *Proceedings, International Symposium on Innovative Numerical Analysis in Applied Engineering Science* (1977) to appear.

5. Gross B., et alia, NASA TND-2395 (1961); TND-2603 (1965); TND-3092 (1965); TND-3295 (1966); *International Journal of Fracture Mechanics* 4 (1968) 267-276.

6. Chan, S. K., I. S. Tuba, and W. K. Wilson, *Engineering Fracture Mechanics* 2 (1970) 1-17; D. G. Smith and C. W. Smith, *International Journal of Fracture Mechanics* 6 (1970) 305-318; R. D. Henshell and K. G. Shaw, Crack Tip Finite Elements are Unnecessary, University of Nottingham (1973) - see also *International Journal of Numerical Methods in Engineering* 10 (1975) 495-507; R. S. Barsoum, *International Journal of Fracture* 10 (1974) 603-605; J. M. Bloom, *International Journal of Fracture* 11 (1975) 705-707.

7. Swedlow, J. L., Development of the Program SPECEL, A Special Element for Elasto-Plastic Crack Tip Stress Analysis, Report SM 74-10, Carnegie-Mellon University (1974).

8. Fung, Y. C., *Foundations of Solid Mechanics*, Prentice-Hall, Edgewood Cliffs (1965) Chapters 10-12.

9. Hein, V. L. and F. Erdogan, *International Journal of Fracture Mechanics* 7 (1971) 317-330.

10. Hutchinson, J. W., *Journal of the Mathematics and Physics of Solids* 13 (1968) 13-31; J. R. Rice and G. Rosengren, *ibid.* 1-12.

11. Swedlow, J. L. and M. E. Karabin, Jr., *Proceedings, Fourth International Conference on Fracture*, University of Waterloo Press (1977) to appear.

12. Karabin, Jr., M. E., Ph.D. Thesis, Department of Mechanical Engineering, Carnegie-Mellon University (1977) in preparation.

13. Jones, D. P., Ph.D. Thesis, Department of Mechanical Engineering, Carnegie-Mellon University (1973) - see also *International Journal of Fracture* 11 (1975) 897-914.

14. Swedlow, J. L., *International Journal of Non-Linear Mechanics* 3 (1968) 325-336; 4 (1969) 77; *Computers and Structures* 3 (1973) 879-898.

15. Marino, C., Ph.D. Thesis, Department of Mechanical Engineering, Carnegie-Mellon University (1977) in preparation.

16. Riccardella, P. C. and J. L. Swedlow, in *Fracture Analysis*, STP 560, American Society for Testing and Materials, Philadelphia (1974) 134-154.

17. Knowles, J. K. and E. Sternberg, An Asymptotic Finite Deformation Analysis of the Elastostatic Field Near the Tip of a Crack, TR 27, California Institute of Technology (1973).

18. Osias, J. R., NASA CR-2199 (1973); *International Journal of Solids and Structures* 10 (1974) 321-339; unpublished research (1975).

19. Osias, J. R., A Finite Element Formulation for Evaluation of Crack Blunting Effects in Elasto-Plastic Solids, Report SM 75-7, Carnegie-Mellon University (1975).

20. Sneddon, I. N., *Proceedings of the Royal Society* (London) A187 (1946) 229-260; R. A. Sack, *Proceedings of the Physical Society* (London) 58 (1946) 729-736.

21. Swedlow, J. L. and M. A. Ritter, in *Stress Analysis and Growth of Cracks*, STP 513, American Society for Testing and Materials, Philadelphia (1972) 79-89.

22. Swedlow, J. L., Stresses near Notches and Cracks with Curved Fronts: Problem Formulation, Report SM 73-18, Carnegie-Mellon University (1972).

23. Southwell, R. V., *Proceedings of the Royal Society* (London) A180 (1942) 367-396.

24. Zak, A. R., *Journal of Applied Mechanics* 39 (1972) 501-506.

25. Irwin, G. R., in *Structural Mechanics*, Pergamon Press, Oxford (1960) 557-594.

26. Neale, B. K., *International Journal of Fracture* 12 (1976) 499-502; RD/B/N3787, Central Electricity Generating Board (1976).

27. Folias, E. S., *Journal of Applied Mechanics* 42 (1975) 663-674.

28. Cruse, T. A., in *Boundary-Integral Equation Method: Computational Applications in Applied Mechanics* AMD-11, American Society of Mechanical Engineers, New York (1975) 31-46.

29. Freese, C. E. and D. M. Tracey, *International Journal of Fracture* 12 (1976) 767-770.

30. Swedlow, J. L. and M. L. Williams, A Review of Recent Investigations into Fracture Initiation at GALCIT, ARL 64-175, USAF Office of Aerospace Research (1964).

31. Emery, A. F., F. J. Cupps, and P. K. Neighbors, in *Computational Fracture Mechanics*, American Society of Mechanical Engineers, New York (1975) 35-48.

32. Akin, J. E., *International Journal for Numerical Methods in Engineering* 10 (1976) 1249-1259.

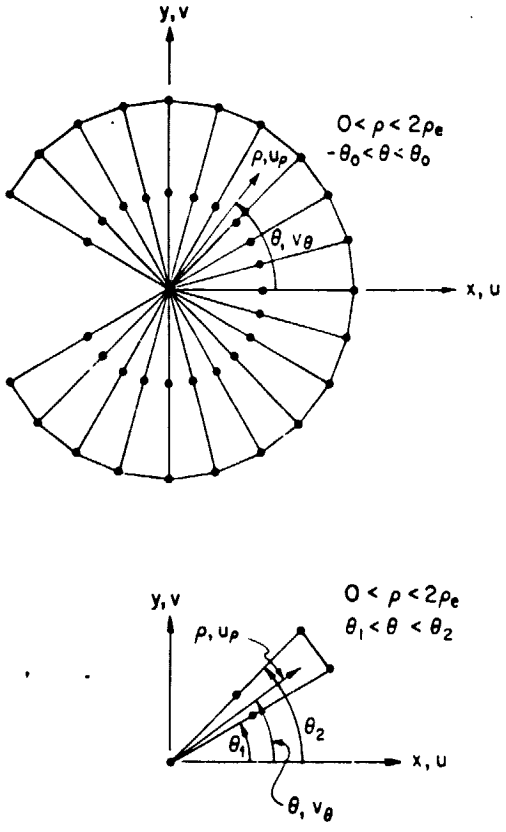


Figure 1, showing a special element comprising twenty sectors and a typical sector with details of coordinates, displacement components, and dimensions.

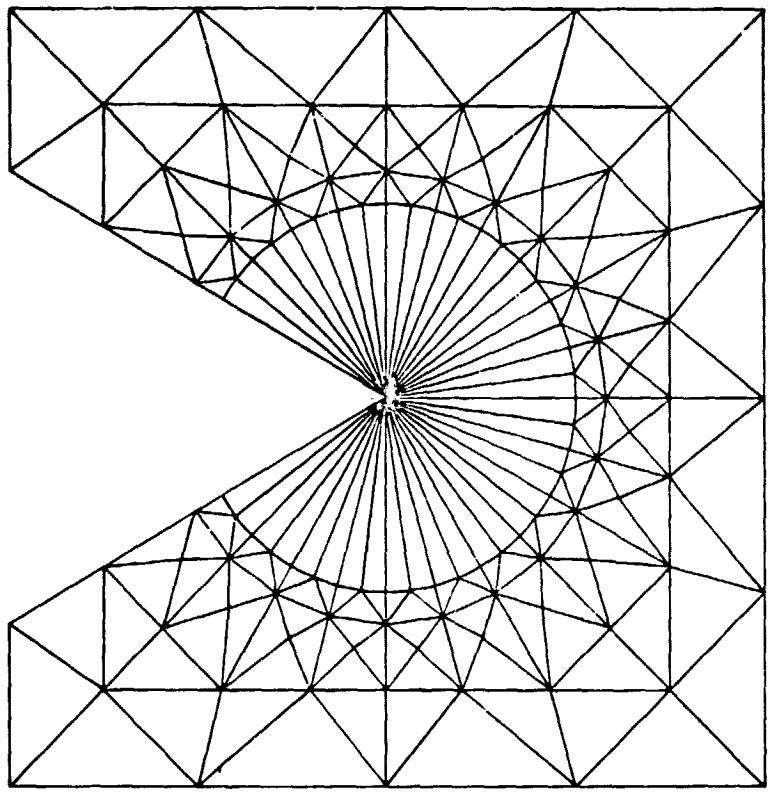

Figure 2, showing a special element embedded in regular elements, CSE formulation.

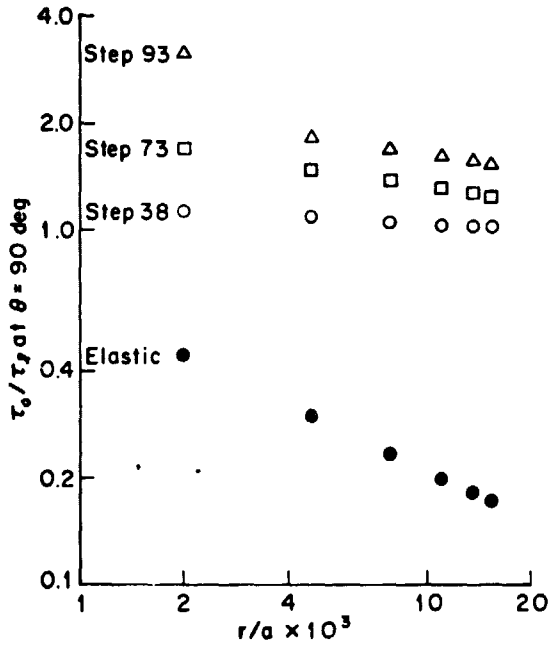


Figure 3, showing radial variation of octahedral stress normalized on limit value (at which yield initiates) at $\theta$ = 90 deg for four load levels; data from problem reported in [11].

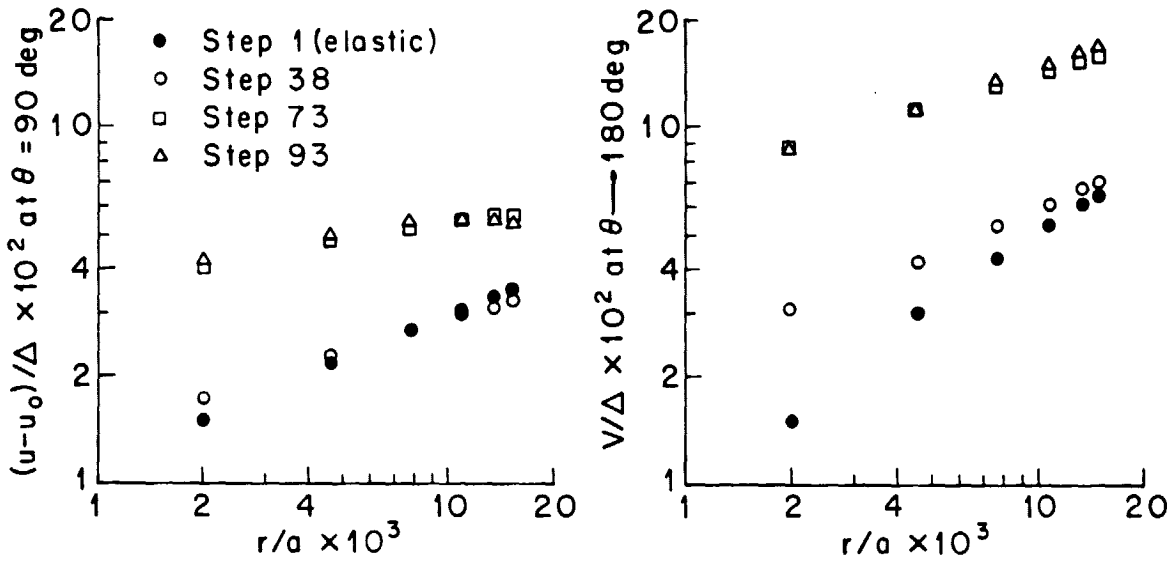


Figure 4, showing radial variation of $(u - u_o)/\Delta$ at $\theta = 90$ deg and $v/\Delta$ at $\theta \rightarrow 180$ deg for four load levels; from [11].

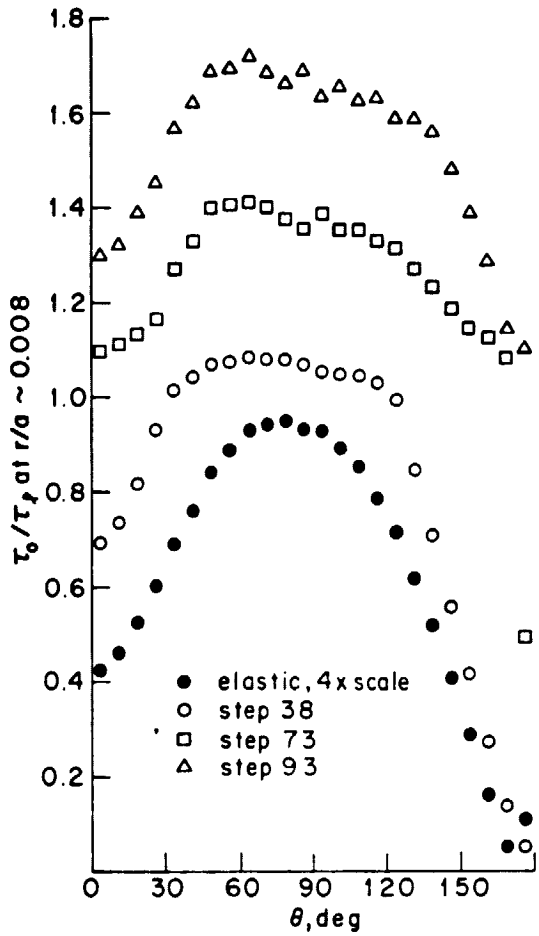


Figure 5, showing angular variation of octahedral stress (normalized on limit value) at r/a $\sim$ 0.008 for four load levels; data from problem reported in [11] (note 4x magnification of elastic results).

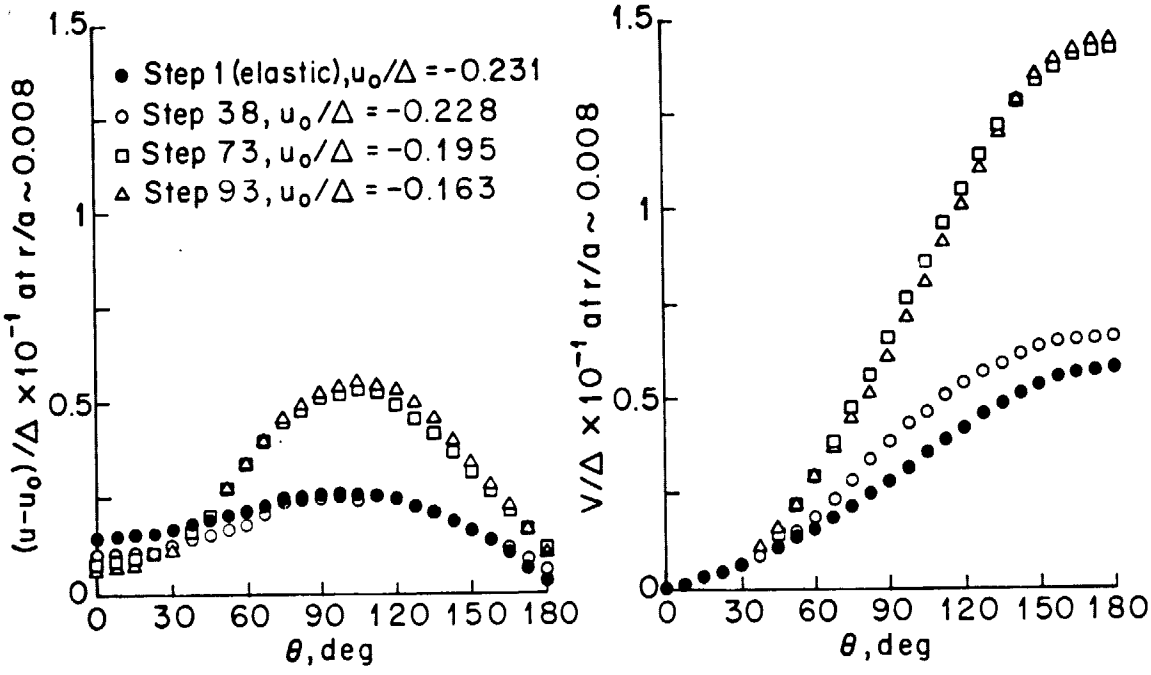


Figure 6, showing angular variation of normalized nodal displacements at r/a $\sim$ 0.008 for four load levels; from [11].

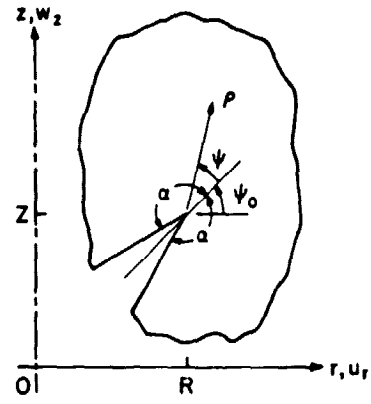


Figure 7, showing coordinates $\rho,\psi$ centered at notch vertex in an axisymmetric coordinate system r,z. Note that origin for $\rho$ is at R,Z and that $\psi = 0$ bisects (interior) notch angle $2\alpha$.

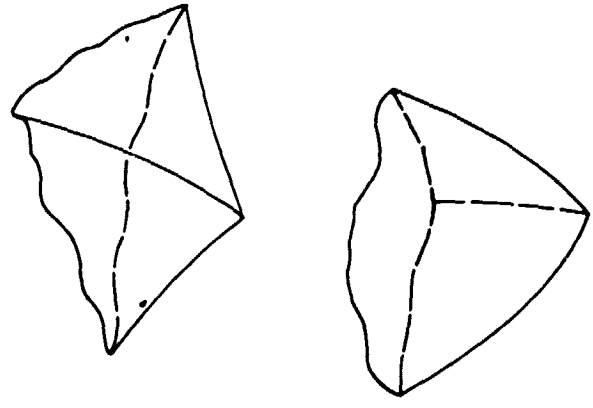

Figure 8, showing cusp-like and re-entrant vertices in three dimensions, formed by intersection of three smooth surfaces.

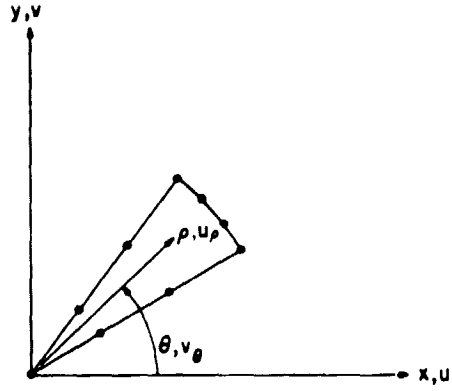


Figure 9, showing an example of a sector in a more refined special element. Details are presumed to follow the pattern shown in Figure 1.